NÖHÜ Müh. Bilim. Derg. / NOHU J. Eng. Sci., 2022; 11(4), 888-897

Niğde Ömer Halisdemir Üniversitesi Mühendislik Bilimleri Dergisi
Niğde Ömer Halisdemir University Journal of Engineering Sciences

Araştırma makalesi / Research article

www.dergipark.org.tr/tr/pub/ngumuh / www.dergipark.org.tr/en/pub/ngumuh

Array gain analyses of MIMO systems in 5G communication systems

5G iletişim sistemlerinde ÇGÇÇ sistemlerin dizin kazanç analizleri

Ural Mutlu[1,*], Yasin Kabalcı[2]

[1] *Niğde Ömer Halisdemir University, Bor Vocational School, 51700, Bor, Niğde Turkey*
[2] *Niğde Ömer Halisdemir University, Electrical and Electronic Engineering Department, 51240, Niğde, Turkey*

Abstract

In the last decade, Multiple-Input Multiple-Output (MIMO) algorithms have been developed for mobile communication networks in order to increase spectrum efficiency and reduce transmitted power, which are also two of the main Key Performance Indicators of Fifth Generation New Radio (5G NR). Therefore, various MIMO algorithms are being researched for their adaptability to 5G NR specifications. The objective of this study is to examine the array gains achieved with the deployment of multiple transmit antennas and multiple receive antennas in 5G NR Physical Downlink Shared Channel (PDSCH). The study first examines the array gains of Single-Input Multiple-Output (SIMO) and Multiple-Input Single-Output (MISO), then combines the transmitter and the receiver diversities in a MIMO system for 5G PDSCH. The array gains are achieved through precoding and combining vectors obtained by Singular Value Decomposition (SVD) of the channel coefficients matrix. The results show that theoretical array gains can be achieved in end-to-end 5G NR downlink channels.

Keywords: Array gain, 5G, MIMO, SIMO, MISO

Öz

Son on yılda, mobil iletişim ağlarında spektrum verimliliğini artırmak ve kullanılan iletim gücünü azaltmak için Çoklu Giriş Çoklu Çıkış (ÇGÇÇ) algoritmaları geliştirilmiştir. Spektrum verimliliğini artırmak ve kullanılan iletim gücünü azaltmak Beşinci Nesil Yeni Radyonun (5G YR) da Temel Performans Göstergelerinden olduğundan MIMO algoritmalarının 5G YR spesifikasyonlarına uygunluğu araştırılmaktadır. Bu çalışmanın amacı, 5G YR Fiziksel Aşağı Yönlü Bağlantı Paylaşımlı Kanalında (FAYBPK) çoklu verici antenler ve çoklu alıcı antenler kullanılarak elde edilen dizin kazançlarını incelemektir. Çalışma, Tekli Giriş Çoklu Çıkış (TGÇÇ) ve Çoklu Giriş Tekli Çıkış (ÇGTÇ) dizin kazanımlarını inceler, ardından 5G YR FAYBPK ÇGÇÇ sisteminde verici ve alıcı çeşitliliklerini birleştirir. Dizin kazanımları, Tekil Değer Ayrıştırma (TDA) ile elde edilen ön kodlama ve birleştirme vektörlerini kullanılarak elde edilir. Çalışma sonuçlara göre teorik dizi kazanımları baştan-uca 5G YR aşağı bağlantı kanallarında elde edilebilmektedir.

Anahtar kelimeler: Dizin kazanç, 5G, ÇGÇÇ, TGÇÇ, ÇGTÇ

1 Introduction

The deployment of Multiple-Input Multiple-Output (MIMO) communication techniques to the mobile communication networks has gained considerable attention in the last decade mainly due to the development in the MIMO processing algorithms, the improvements in the computing capabilities of the mobile devices, and the increase in carrier frequencies. The term MIMO is used to describe both a communication system consisting of an array of multiple transmit and receive antennas and the signal processing algorithms involved in the successfully transmission of modulated signals through these multiple antennas. MIMO improves the reliability, power consumption, and spectral efficiency of communication systems by providing spatial diversity and spatial multiplexing [1–3]. Spatial diversity uses the spatially separated multiple channels between transmit and receive antennas to improve the reliability and the power consumption of a single data stream. Spatial multiplexing, on the other hand, uses the multiple signal paths to send multiple data streams simultaneously in order to increase spectral efficiency.

MIMO has been successfully deployed in various wireless communication systems such as IEEE 802.11n/ac [4, 5], IEEE 802.16 [6], Fourth Generation Long-Term Evolution (4G LTE) [7], Fifth Generation New Radio (5G NR) [8], etc. The first introduction of MIMO to mobile communication networks was with the 3rd Generation Project Partnership (3GPP) Release 7, where the Base Stations (BS) supported 2x2 MIMO but it had limited success [9]. The real benefits of MIMO were realised with the introduction of Orthogonal Frequency Division Multiplexing (OFDM) in 3GPP Release 8 for 4G LTE. MIMO in LTE also started as a 2x2 MIMO supported only by the base station, whereas the latest version of LTE, Release 14, supports 8x8 MIMO in the downlink and 4x4 MIMO in the uplink directions [7]. Following the success of LTE, 3GPP Release 15 specifies 5G NR, where the deployment of massive MIMO (mMIMO) antenna arrays of size 64 and upwards at the BS would facilitate the use of new MIMO algorithms. Furthermore, the increase in the frequency range decreases the wavelength leading to smaller antenna array size in the transceivers of the User Equipment (UE). The transition from limited MIMO in LTE to mMIMO will be the defining characteristic

* Sorumlu yazar / Corresponding author, e-posta / e-mail: uralmutlu@gmail.com (U. Mutlu)
Geliş / Recieved: 15.03.2022 Kabul / Accepted: 06.07.2022 Yayımlanma / Published: 14.10.2022
doi: 10.28948/ngmuh.1088264

of 5G NR. Therefore, there are lots of research projects focusing on MIMO techniques in 5G NR [10–12].

Most of the MIMO algorithms in wireless communications rely on the multipath nature of the wireless channel, which results in spatial diversity. It is generally assumed that independent and identically distributed multipath channels have low correlation and the likelihood that all the channels suffer deep fade at the same time is also low [1–3]. Therefore, coherent combination of multiple channels in a constructive manner at the transmitter and the receiver leads to the spatial processing gains of array gain and diversity gain [3, 11]. Array gain is defined as the increase in the ratio of the average Signal to Noise Ratio (SNR) obtained by combining multiple antenna signals in MIMO transmission to the SNR of a Single-Input-Single-Output (SISO) transmission. Whereas, diversity gain is the degree of increased reliability due to the use of independently fading paths.

[13] is one of the first studies to formulate capacities and error exponents of MIMO communication system. Since then, the capacity and the power gains of MIMO algorithms have been well-established [1–3, 11]. In MIMO transmission, the combination of the multiple signals is carried out by multiplying the signals of the antenna array elements with complex precoding and combining vectors at the transmitter and the receiver. Precoding and combing of the multiple paths at RF chain level is also termed as digital beamforming. The optimum precoding and combining algorithms for a Single User MIMO (SU-MIMO) are the Maximum Ratio Transmission (MRT) and the Maximum Ratio Combining (MRC) methods, both of which use Singular Value Decomposition (SVD) to obtain the precoding and combining vectors [11, 14].

In a comprehensive study, [15] compares various linear precoding techniques for Multi-User MIMO (MU-MIMO) transmission in 5G NR and the results show that in case of digital beamforming MRT performs better than Zero Forcing (ZF) at lower SNR values but worse than MMSE. This shows that the MRT is a viable solution for improving SNR when the power is minimal. In a similar study on energy efficiency for MU-MIMO transmission in 5G NR, [16] also confirms that the combination of MRT and MRC improves the energy efficiency at lower SNR values better than ZF and has a similar performance to MMSE. [17] is another study on energy efficiency for MU-MIMO transmission and the results show that MRT has a better energy efficiency than ZF when the number of antennas at the BS is not too high. [18] simulates a MU-MIMO with 32 transmit antennas and 110 moving receivers in order to compare MRC, Selection Combining, and Equal Gain Combining algorithms. The results of the study show that the combination of the MRT and MRC provides the best performance. Although, MRT and MRC are not 5G specific algorithms, the research on 5G NR MIMO confirms that MRT and MRC are applicable in transmissions where the number of users is not high [19], [20]. MRT and MRC also have the advantage of being the easiest to implement and deploy [21].

Despite the large body of research on MU-MIMO algorithms in 5G NR [15], not many studies investigate the SNR improvements that can be achieved by MRT and MRC in 5G NR physical channels for a SU-MIMO scenario [22]. In 5G NR Physical Downlink Shared Channel (PDSCH), for precoding without codebook, the requirement is that the precoding and combining are made transparent to the UE and BS [23]. From the BS's perspective, the PDSCH transmission is a Multiple-Input Single-Output (MISO) transmission and the receiver is not aware of the multiple transmit antennas. Similarly, the UE views the transmission as a Single-Input Multiple-Output (SIMO) transmission. Moreover, without a shared codebook, spatial multiplexing is not applicable. Thus, a simple PDSCH without codebook precoding can be thought as a single stream SU-MIMO transmission. Therefore, the aim of this study is to investigate the array gain improvements that can be achieved by the deployment of multiple antennas at the BS and the UE when codebooks are not used in 5G NR PDSCH transmission.

To this end, the study establishes 5G NR PDSCH channel with MRT precoding at the transmitter and MRC combining at the receiver. First, the effects of the precoding vector on the array gain in MISO transmission and the effects of combining vector on the array gain in SIMO transmission are investigated. Then, the transmit antenna and receive antenna diversities are combined and the array gain for MIMO transmission is examined. The study uses 3GPP specified Tapped Delay Line (TDL) channel model.

The rest of the paper is organised as follows, section 2 describes the processes of precoding and combining, and then it establishes the equations and the bounds for the array gains. Section 3 gives an outline of the 5G NR PDSCH specifications as well as the specifications for the TDL channel model. Section 4 shows the simulation results as Bit Error Rate (BER) plots for SIMO, MISO, and MIMO separately. Finally, the last section is the conclusion section summarising the experiences acquired during the project.

The notations and assumptions used in this paper are as follows. Matrixes are represented with capital letters, for example A. Vectors are given with small bold letters, e.g. $\mathbf{a}$. $(.)^{T}$ and $(.)^{*}$ are transpose and conjugate operations and $(.)^{H}$ is the Hermitian matrix operation.

2 MIMO array gain analysis

Figure 1 shows the reference model for a SU-MIMO transmission. In this model, the transmitter is equipped with N_t antennas and the receiver, similarly, has N_r antennas. $H \in C^{N_r \times N_t}$, the channel matrix, describes the attenuations and the phase shifts of the air interface between transmitter and receiver antenna pairs. The elements of the channel matrix are given as h_{ij}, where i indexes the receiver antenna and j is the transmitter antenna index. Each channel is also assumed to be a multipath channel with different paths arriving at the receiver with different delays, attenuations, and phases. The analysis in this section are based on the assumption that channel estimation is carried successfully and that both the transmitter and receiver have almost perfect Channel State Information (CSI).

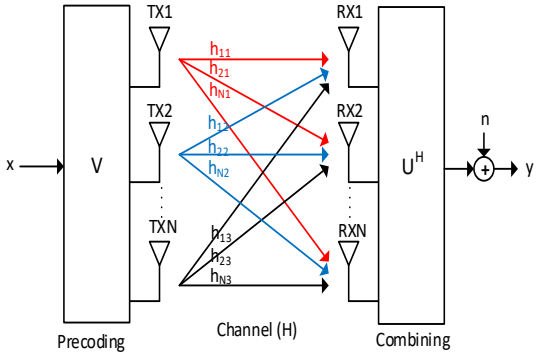

Figure 1. Reference model for single user MIMO transmission

2.1 *Precoding and combining with SVD*

Since, the aim of the study is to observe the power gains in SNR, the optimum algorithms of MRT and MRC were chosen for this study. MRT precoding and MRC combining methods are based on the principal right and left singular vectors of the SVD and the vectors can achieve full array gain in MISO and SIMO transmission modes regardless of the channel correlations. However, when the MRT and MRC are employed at the same time, the result would be dependent on the channel correlations. The SVD decomposes the channel matrix H as [1, 3]:

$$H = UDV^H \tag{1}$$

Where $D = diag(s_1, s_2, \ldots, s_i)$ is a diagonal matrix containing real valued singular values in order from the maximum to the minimum, $s_1 > s_2 > \ldots > s_i$. The dimensions of D or the number of singular values is limited by the rank of H, given as $rank(H) = \min(N_r, N_t)$ assuming the correlation between the channels is relatively low. U and V are unitary matrixes of size $N_r \times N_r$ and $N_t \times N_t$ respectively. They are unitary matrixes in a sense that the multiplication of the matrix with its Hermitian is an identity matrix, as in $UU^H = I$ and $VV^H = I$. The vectors of the V matrix are employed as precoding vectors and the vectors of the U^H matrix are the combining vectors. V and U can be represented as $[\mathbf{v}_1, \mathbf{v}_2, \ldots, \mathbf{v}_t]$ and $[\mathbf{u}_1, \mathbf{u}_2, \ldots, \mathbf{u}_r]$. The **v** and **u** vectors are orthonormal vectors, in other words, their norms are 1 and the inner products of the **v** and the **u** vectors results in 0. For a single user, it is always the first vectors of the matrices and the first singular value that are used for precoding and combining.

The analyses for a single layer transmission are as follows. Given that x is the complex valued modulated symbol sent through the channel with the coefficients given in H, the received signal y with the noise added at the receiver is:

$$y = Hx + n \tag{2}$$

Where, n is Additive White Gaussian Noise (AWGN), $n \sim CN(0, \sigma^2)$ added at the receiver before applying the combining algorithm. The H matrix in Equation 2 can be replaced with SVD decomposed matrices to give:

$$y = UDV^H x + n \tag{3}$$

Mathematically speaking, by applying the precoding vector $\mathbf{v_1}$ at the transmitter, the effects of V^H are cancelled out. Likewise, at the receiver the combining vector $\mathbf{u_1^H}$ would also cancel out the effects of the U matrix, leaving only the singular values in the equation. Applying the precoding and combining vector, the equation for the received signal becomes:

$$y = \mathbf{u_1^H}\left(UDV^H \mathbf{v_1} x + \mathbf{n}\right) \tag{4}$$

By replacing both the V^H and U matrices with the vectors and using 2x2 MIMO as an example, Equation 4 can be rewritten as:

$$y = \mathbf{u_1^H}\left(\begin{bmatrix}\mathbf{u_1} & \mathbf{u_2}\end{bmatrix}\begin{bmatrix}s_1 & 0\\ 0 & s_2\end{bmatrix}\begin{bmatrix}\mathbf{v_1^*}\\ \mathbf{v_2^*}\end{bmatrix}\mathbf{v_1} x + \mathbf{n}\right) \tag{5}$$

Thus the resulting received signal can simply be shown as:

$$y = s_1 x + \mathbf{u_1^H n} \tag{6}$$

The $\mathbf{u_1^H}$ multiplier in the noise term can be ignored as $\mathbf{u_1^H}$ is orthonormal and would not have an effect on the expected value of noise. Equation 6 is the general equation for a single stream SU-MIMO. Equation 4 and 5 can also be applied for transmission of multiple streams or layers by using the other vectors and singular values of the SVD matrices. The equation for an i^{th} user or stream can be rewritten as:

$$y = s_i x_i + n \tag{7}$$

The equation shows that the received signal is the transmitted signal multiplied with the singular value of the channel coefficients matrix. This is the property of SVD that is used in spatial multiplexing, which is not in the scope of this study.

2.2 *Array gain analyses*

In order to calculate the array gain, first the SNR of SISO transmission is established and then MISO, SIMO, and MIMO transmission SNRs are given as ratio of SISO SNR. For simplicity of analysis, the average transmitted symbol energy and the expected value of the noise variance are assumed to be equal to 1.

2.2.1 SISO SNR

In SISO transmission, the transmitted signal goes through a multi-path fading channel with a channel coefficient of h and at the same time suffers AWGN noise, which is modelled as an addition at the receiver. The received signal y and its corresponding SNR are given as:

$$y = hx + n \tag{8}$$

$$SNR = |h|^2 \tag{9}$$

2.2.2 MISO Array Gain

Since, MISO is a $N_t \times 1$ transmission scheme, $\mathbf{u_1}$ is 1 and the channel decomposition is equal to $\mathbf{h} = s_1.\mathbf{v_1}^{\mathbf{H}}$. The precoding vector and the resulting received signals after precoding and noise are added are:

$$\mathbf{v_1} = \frac{\mathbf{h}^*}{s_1} \tag{10}$$

$$y = \mathbf{h}^{\mathbf{T}} \frac{\mathbf{h}^*}{s_1} x + n \tag{11}$$

For a vector, its singular value is also its L_2 norm; therefore, Equation 11 can be rewritten as:

$$y = \mathbf{h}^{\mathbf{T}} \frac{\mathbf{h}^*}{\|\mathbf{h}\|} x + n \tag{12}$$

$$y = \|\mathbf{h}\| x + n \tag{13}$$

Equations 12 and 13 are also the equations used to describe MRT precoding [24, 25]. From Equation 13, the SNR of MISO transmission can be simply calculated as:

$$SNR = \|\mathbf{h}\|^2 \tag{14}$$

Where, $\|\mathbf{h}\|^2$ is the sum of the squares of the channel coefficients of the individual SISO channels that make up the MISO transmission. Assuming h_i is the channel coefficient of the i^{th} SISO channel, the SNR of MISO becomes:

$$\|\mathbf{h}\|^2 = \sum_{i=1}^{N_t} |h_i|^2 \tag{15}$$

Provided channel gains are normalised and averaged, it can be assumed that $\|\mathbf{h}\|^2$ averages to $N_t \times |\mathbf{h}|^2$. Therefore, the SNR and the array gain of a MISO transmission would be:

$$SNR_{MISO} = N_t \times SNR_{SISO} \tag{16}$$

Thus, the array gain for MISO transmission is equal to the number of transmitter antennas, N_t.

2.2.3 SIMO array gain

The channel decomposition for a single layer SIMO, assuming $\mathbf{v_1} = 1$, becomes $\mathbf{h} = \mathbf{u_1} s_1$. By replacing s_1 with $\|\mathbf{h}\|$, the combing vector $\mathbf{u_1}^{\mathbf{H}}$ becomes:

$$\mathbf{u_1}^{\mathbf{H}} = \frac{\mathbf{h}^{\mathbf{H}}}{\|\mathbf{h}\|} \tag{17}$$

Since, there is no precoding in SIMO transmission, the received signal after applying the combining vector is given with:

$$y = \frac{\mathbf{h}^{\mathbf{H}}}{\|\mathbf{h}\|} (\mathbf{h}x + \mathbf{n}) \tag{18}$$

$$y = \|\mathbf{h}\| x + \frac{\mathbf{h}^{\mathbf{H}}}{\|\mathbf{h}\|} \mathbf{n} \tag{19}$$

The SNR of the received signal in Equation 19 can be calculated as in Equation 20:

$$SNR = \frac{\|\mathbf{h}\|^2}{\frac{\mathbf{h}^{\mathbf{H}}\mathbf{h}}{\|\mathbf{h}\|^2}} = \|\mathbf{h}\|^2 \tag{20}$$

The equation for SNR for the received signal in SIMO is the same as Equation 16 and can be shown as:

$$SNR_{SIMO} = N_r \times SNR_{SISO} \tag{21}$$

From the Equation 21 the array gain for SIMO transmission is equal to the number of receive antennas, N_r.

2.2.4 MIMO array gain

The exact value of the array gain in MIMO depends on the nature of the channel coefficients and its analyses is not as straight forwards as in MISO and SIMO [11, 25]. However, it is possible to establish an upper bound for the array gain and understand the conditions that can lead to the upper bound.

For the MIMO SNR analysis, the received signal in Equation 6 is used and the equation shows that the

transmitted signal is simply multiplied by the first singular value. To get the upper bound, the analyses make use of the Frobenius norm of the channel coefficients matrix. The Frobenius norm of a channel coefficients matrix is the square root of the sums of the squares of absolute values of each matrix coefficient, shown in Equation 22. In other words, the square of the Frobenius norm can be thought as the sum of match filtered SISO channels [25, 26]. This would also denote the total power that can be transmitted using all the SISO channels available. If the average value of $\left|h_{ij}^{*}.h_{ij}\right|$ is assumed to be $\left|h\right|^2$, as in SISO transmission, the square of the Frobenius norm would be equal to the sum of $N_r \times N_t$ SISO channels, Equation 23:

$$\left\|H\right\|_F^2 = \sum_{i=1}^{N_r}\sum_{j=1}^{N_t}\left|h_{ij}^{*}.h_{ij}\right| \tag{22}$$

$$\left\|H\right\|_F^2 = N_r N_t \left|h\right|^2 \tag{23}$$

$$\left\|H\right\|_F^2 = \sum_{i=1}^{rank(H)} s_i^2 \tag{24}$$

Another property of the Frobenius norm is that the square of the Frobenius norm is the sum of the squares of the singular values, Equation 24. From Equation 7, the SNR of each stream or layer in spatially multiplexed MIMO is proportional to the square of its singular value. Therefore, the square of the Frobenius norm can be interpreted as sharing of the available power between multiple layers, where each layer's share is proportional to the square of its singular value. The SNR for a single layer SU-MIMO is thus:

$$s_1^2 = N_r N_t \left|h\right|^2 - \sum_{i=2}^{rank(H)} s_i^2 \tag{25}$$

In order to intuitively deduce an upper bound for the array gain for a single layer MIMO, the extreme case of a channel where all the coefficients are equal or *Rank(H)=1* could be considered, as is the case in both SIMO and MISO. In this scenario, s_1 reduces to $s_1^2 = N_r N_t \left|h\right|^2$ and the resulting array gain bounds become [25]:

$$max\{Nr, Nt\} \le AG \le N_r N_t \tag{26}$$

The upper bound of Equation 26 is not very realistic as it represents the array gain for MIMO transmission with highly correlated channels. In highly correlated channels, the square of the first singular value is much larger than the total of the squares of the other singular values. Therefore, the Frobenius norm would be *dominated* by the first singular value and the array gain would be close to $N_r \times N_t$. Using SVD based MRT and MRC to calculate precoding and combining vectors is therefore also referred to as Dominant Eigenmode Beamforming or Maximum Eigenmode Beamforming.

In uncorrelated channels or in channels with lower correlation, the dominance of the first singular value would reduce, and the array gain for such uncorrelated channels has been shown to be upper bounded by [27]:

$$AG \le \left(\sqrt{N_r} + \sqrt{N_t}\right)^2 \tag{27}$$

In summary, the array gain of a SU-MIMO would depend on the channel properties. The channel model used in this research is TDL channel model, where each channel is multipath fading channel and the correlation between the channels is low. Therefore, the upper bound for the array gain given in Equation 27 would be the expected result.

2.2.5 Zero forcing receiver

The analyses in the previous sub-sections are based on MRC, which is a Matched Filter (MF) receiver. In MF receivers, the received signal is multiplied with H^H and the output of the receiver is a scaled version of the received signal as given in Equation 13 and 19. However, the received signal needs to be normalised before further processing. The receiver implemented in this study is a ZF receiver, which is designed to eliminate the effects of the channel coefficients by multiplying the channel coefficients with the inverse of the channel, thus also eliminating the need for normalising the power. For the purposes of this study, ZF and MF would produce comparable results and the assumption that MRC produces optimum results for SU-MIMO is still satisfied.

The combining matrix for the ZF receiver can be shows with the pseudo-inverse of the channel coefficients:

$$W_{ZF} = \left(H^H H\right)^{-1} H^H \tag{28}$$

In Equation 28, the H matrix seen by the receiver is not the full channel coefficients matrix but the precoded version of the matrix. The channel coefficients matrix seen by the receiver is termed as the effective channel coefficients matrix, H_{eff}, and is given as:

$$H_{eff} = UDV^H V = UD \tag{29}$$

Replacing the matrices with vectors and singular values, such that $\mathbf{h_{eff1}} = \mathbf{u_1}.s_1$, the combining vector for a ZF receiver can be rewritten as:

$$\mathbf{w_{ZF}} = \frac{\left(\mathbf{h_{eff1}}\right)^H}{\left(\mathbf{h_{eff1}}\right)^H.\mathbf{h_{eff1}}} \tag{30}$$

$$\mathbf{w_{ZF}} = \frac{\mathbf{u_1^H}}{s_1} \tag{31}$$

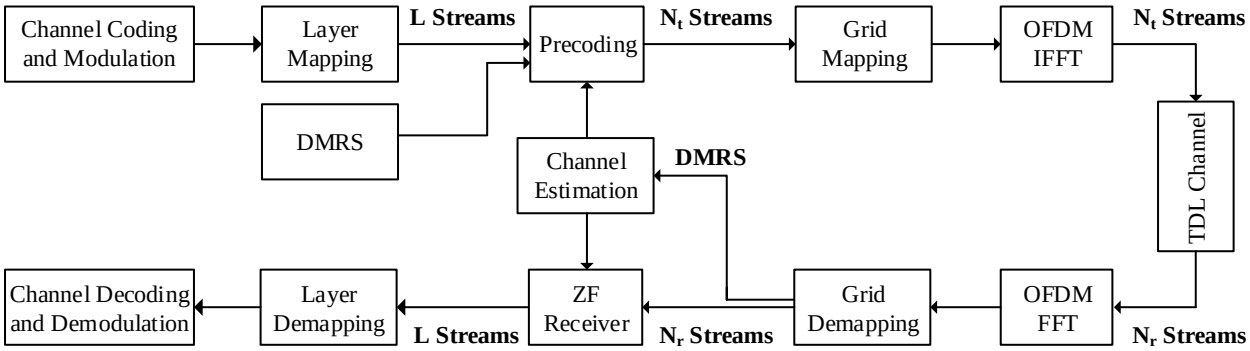

Figure 2. 5G NR PDSCH MIMO processing block diagram

As the Equation 31 shows, the ZF receiver vector is a scaled version of the MF combining vector. If ZF receiver is used instead of MF, Equation 6 would become:

$$y = x + \frac{\mathbf{u}_1^{\mathbf{H}}}{s_1}\mathbf{n} \tag{32}$$

Incidentally, Equation 32 would give the same array gain results as in the previous analysis.

3 5G NR PDSCH processing chain and TDL channel model

Conceptually, the data processing procedures of PDSCH are divided into two stages; multiplexing and channel coding stage and physical channels and modulation stage which are defined in [28] and [23] respectively. Although, the simulations of the study implement all the procedures, the focus of the research is on the MIMO related steps, which start after channel coding and modulation. Figure 2 shows the block diagram for the procedures that are explained in this section.

The processes in the Channel Coding and Modulation block, shown in Figure 2, are applied to the data in the transport blocks arriving from the Medium Access Control (MAC) layer. These processes are in the following order: CRC Attachment, block segmentation, Low Density Parity Check (LDPC) encoding, Rate Matching and Interleaving, and Modulation. After modulation, MIMO related procedures of Layer Mapping, Precoding, Grid Mapping, and OFDM modulation are applied to the modulated code words.

3.1 Layer mapping

Layer Mapping is the process of splitting the modulated complex valued symbols into multiple streams and mapping each stream to a layer. In 5G terminology, the term layer refers to the number of streams that are spatially multiplexed to achieve higher spectral efficiency. The current study investigates a single layer transmission; therefore, data is not divided into multiple layers.

3.2 Precoding

Precoding is the step where modulated complex valued symbols are precoded and mapped to antenna. Precoding is a serial to parallel converter through which a single symbol for a given layer is mapped on multiple antennas with amplitude and phase determined by the precoding vector. According to [29], the requirement for the coherent combination of the antenna array outputs is that any precoding algorithm should be transparent to the UE. Therefore, the precoding method or matrix that is applied to the user data is also applied to the Demodulation Reference Signal (DMRS), Figure 2. The application of the precoding matrix to the DMRS hides the precoding matrix within the channel estimate. In other words, the channel seen by the receiver is the effective channel given with Equation 29.

3.3 Grid mapping and OFDM modulation

The precoded complex symbols are then mapped on to the resource elements in two stages. In the first stage, symbols are mapped onto “virtual resource blocks”, which is an array of blocks marked as available for transmission. The symbols are then mapped from the virtual resource blocks to “physical resource blocks”.

OFDM Modulation is the last step in the transmitter. OFDM Modulation is carried out separately for each transmitter antenna. For baseband analyses, the output of each individual OFDM Modulation is in effect a transmitter antenna signal. Since all the antennas transmit over the same frequency, a channel coefficient is applied to each signal and the signals are then simply superimposed onto one another.

3.4 Receiver and PDSCH decoding

The receiver and the decoding algorithms are the inverse of PDSCH transmitter algorithms, with the exception of channel estimation and MIMO receiver.

3.5 Channel estimation

Channel estimation in 5G NR is achieved through DMRS, which is based on Gold Sequences or Gold Codes [28, 30]. 5G NR specifications define how the DMRS is used by specifying its allocation, mapping type, position in the

resource grid, length, scheduling, etc. To obtain the coefficients, the transmitter assigns a unique DMRS sequence(s) at a unique PDSCH OFDM grid position(s) and each receiver uses the known DMRS sequence to calculate the amplitude and the phase of the received signal. The H matrix obtained through the DMRS would be an estimate rather than an exact matrix.

Moreover, it is generally assumed that MIMO beamforming algorithms use Time Division Duplexing (TDD) mode in which the channel reciprocity principle applies [31, 32]. The reciprocity principle is based on the fact that the channel properties are the same for both downlink and uplink and that channel coefficients can be estimated by the BS through the DMRS sent in the uplink.

3.6 Tapped delay line (TDL) channel model

Wireless communications channels are characterised as multipath fading channels that can cause fluctuations in the received signal's magnitude, phase, and angle of arrival. 3GPP has defined TDL channel models for the multipath environments for frequencies from 0.5GHz up to 100 GHz [32, 33].

The model employs a number of flat fading generators or taps. In the model the taps are independent of each other and generate flat fading Rayleigh distributed channel for Non-Line-of-Sight (N-LOS) paths and Ricean distributed channel for LOS paths. The channel impulse response of the multipath TDL model with N numbers of taps and $a_k(t)$ the amplitude at the τ_k delay for the k^{th} tap is implemented as an FIR filter with the following output:

$$h(t,\tau) = \sum_{k=1}^{N} a_k(t)\delta(t-\tau_k) \tag{33}$$

The TDL channel model is described for SISO systems. For a MIMO model, $N_r \times N_t$ number of SISO channels and a level of correlation between the SISO channels can be defined.

4 Simulations and results

In this section, 5G NR PDSCH is simulated for various transmit and receive antenna configurations. The processing chain described in section 3 and shown in Figure 2 is implemented with the parameters in Table 1.

The channel estimation implemented in the simulations emulates the channel reciprocity principle. The channel coefficients are calculated by averaging the channel coefficients matrix of the received Physical Resource Block (PRB) and are used to calculate ZF receiver vectors. These coefficients are also used to precode the next transmitted PRB. In other words, precoding vectors are obtained from the previously received PRB's channel estimates. On the other hand, for the simulation purposes, the channel coefficients are taken directly from the channel model instead of using the DMRS. Therefore, the channel estimation is perfect. The polarisation mode in the TDL channel model was set to co-polar, which indicates that the antennas transmit with the same polarisation angle and are independent from each other. Finally, the MIMO correlation was set to Low or 0.

Table 1. Simulation parameters

Parameter	Value
Subcarrier Spacing	30kHz
Number of RBs	50
Sample Rate	30,720,000
Modulation	16QAM
LDPC Code Rate	1/2
Channel Estimation	Perfect
Channel Model	TDL-C
Delay Spread	100ns (Nominal DS)
MIMO Correlation	Low - 0
Polarisation	Co-Polar
Simulation Size	200 Frames (~6.10^7 bits)

First, a benchmark BER simulation for SISO was carried out. Then, simulations for MISO, SIMO, and MIMO were run. For all the simulations, BER graphs are plotted and the results are compared.

4.1 MISO array gain results

A MISO transmission system using the parameters in Table 1 was set up and run for antenna configurations of 2x1, 4x1, and 8x1. The simulation results are plotted as BER graph together with the BER for the benchmark of SISO transmission in TDL channel. The results are displayed in Figure 3.

The BER improvements for 2x1 and 4x1 MISO transmission compared to SISO are approximately 3dB and 6dB, which correspond to array gains of 2 and 4 respectively. These results show that array gains are equal to the number of transmit antennas. On the other hand, the array gain for 8x1 MISO is slightly less than the expected 9dB. Overall, the BER simulations for MISO show that keeping all the parameters identical by changing the number of antennas at the transmitter, the required transmit power can be reduced linearly with the number of antennas.

4.2 SIMO array gain results

Similar to MISO, simulations were run for antenna configurations of 1x2, 1x4, and 1x8. BER simulation results are given in Figure 4.

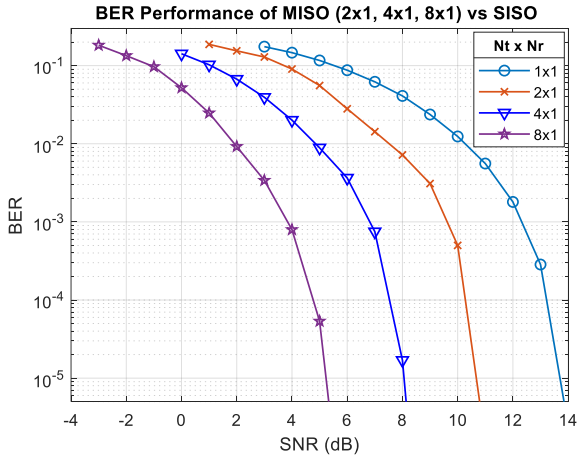

Figure 3. MISO BER simulation results

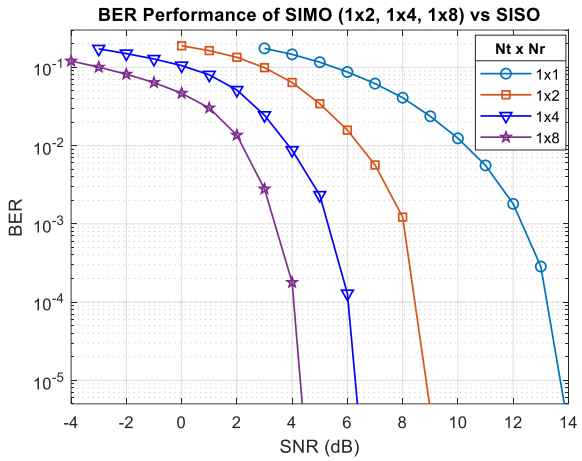

Figure 4. SIMO BER simulation results

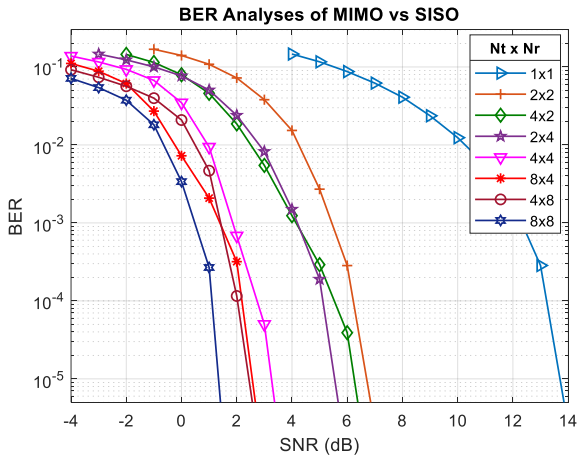

Figure 5. MIMO BER simulation results

The BER improvements for 1x2, 1x4, and 1x8 SIMO transmissions compared to SISO are 5dB, 7.7dB, and 9,8dB respectively, which correspond to array gains of 3.16, 5.88, and 9.54. These results are higher than expected. The results also show that there is a sudden increase in the array gain going from a single antenna to two antennas. Although, 1x4 and 1x8 still perform better than the theoretical values, the improvements for each doubling of the antenna numbers reduces and with 1x8 transmission mode the array gain is closer to the expected value.

The performance difference between MISO and SIMO could be partly explained with the way channel estimation is used. As mentioned at the beginning of the section, MISO uses channel estimation of the previous PRB, while SIMO uses the current PRB's coefficients. Therefore, there is a small time delay in the channel estimates of MISO, which may explain why SIMO performs better than MISO. However, this does not explain why the array gain of SIMO is bigger than N_r.

In [34], Chen offers another reason why the array gain is higher than the number of receive antennas in SIMO. Chen states that SIMO diversity or receive beamforming tends to steer the received beam to the dominant path and spatially filters secondary paths arriving from other directions at later times. In other words, SIMO acts as if the delay spread for the stronger signals has been reduced and as if the coherence bandwidth has been increased. Chen also states that the reduced delay spread and the bandwidth effect have been experimentally verified.

In the array gain analysis of SIMO, it was assumed that the channel responses average over time and that they are equal. However, for SIMO with small number of antennas, it could also be a case where the rule of the averages does not converge. Why SIMO performs better than the theoretical algorithms for smaller number of antennas should be further investigated.

4.3 MIMO array gain results

The BER simulation results for MIMO are displayed in Figure 5 and the power gains compared to SISO transmission are tabulated for better clarity. According to the results given in Table 2, all the array gains are within the bounds specified in Equation 26 and 27 except for 2x2 MIMO, whose upper bound for Equation 26 should be 4. This exception is due to the increase in the array gain for smaller arrays in the receiver side.

Table 2. MIMO simulation results as ratio

N_t x N_r	dB	AG Ratio
2x2	7	5
4x2	7.5	5.6
2x4	8.5	7.1
4x4	10.5	11.2
8x4	11.2	13.2
4x8	11.4	13.8
8x8	12.5	17.8

Figure 5 shows that the array gain goes up with the increase in the number of antennas at the transmitter and the receiver, in other words the array gain of MIMO is affected by both precoding and combing vectors. Furthermore, when 2x4 and 4x2 are compared it is obvious that the number of

receive antennas has a higher effect on the array gain, the same argument can be made for 4x8 and 8x4 transmissions.

Finally, the array gain for the larger antenna array sizes does not increase as much as it does for the smaller arrays. The diminishing returns was also observed in MISO and SIMO transmission modes.

5 Conclusions

The aim of the study was to investigate and simulate the SNR improvements that can be achieved by applying precoding and combining vectors to 5G NR PDSCH. The study first established the theoretical equations for the array gains in MISO and SIMO, which are equal to the number of transmit and receive antennas respectively. Then, the upper bounds for array gain in MIMO scheme were given, which are based on the assumption that in MIMO transmission the correlation of the channels is relatively low.

Simulation of PDSCH for MISO confirmed that array gain improvements are as expected. However, when the same simulation was run for SIMO, the results were higher than the theoretical expectations. It was argued that this discrepancy might be a results of how SIMO modifies the channel properties and these claims should be further investigated. The higher than expected improvements in SIMO also affected MIMO results, where MIMO modes with higher number of receive antennas offered higher array gain. It was also observed that the increase in the array gain reduces as the number of antennas grows. The upper limit for the array gain should also be established in future research.

Finally, according to [35], the radio networks consume more than 60% of the electric power in the mobile networks and this consumption is expected to increase even further with the deployment of 5G NR. Therefore, any array gains would contribute to the reduction of the power consumption both at the base station and at the UE. In summary, the study showed that array gains are achievable for PDSCH in TDL channels.

Conflict of interest

The authors declare that there is no conflict of interest.

Similarity rate (iThenticate): 15%

References

[1] H. Kim, Design and Optimization for 5G Wireless Communications. Wiley-IEEE Press, 2020.
[2] A. Goldsmith, Wireless Communications. Cambridge: Cambridge University Press, 2005.
[3] D. Tse and P. Viswanath, Fundamentals of Wireless Communication. Cambridge University Press, 2005.
[4] IEEE SA, “IEEE 802.11n-2009.” https://standards.ieee.org/ieee/802.11n/3952/. Accessed March 2022
[5] IEEE SA, “IEEE 802.11ac-2013.” https://standards.ieee.org/ieee/802.11ac/4473. Accessed March 2022
[6] IEEE, “IEEE 802.16-2017.” https://standards.ieee .org/ieee/802.16/6996/. Accessed March 2022
[7] 3GPP, “Release 14.” https://www.3gpp.org/release-14. Accessed March 2022
[8] 3GPP, “Release 15.” https://www.3gpp.org/release-15. Accessed March 2022
[9] 3GPP, “Release 7.” https://www.3gpp.org/specifications/releases/73-release-7. Accessed March 2022
[10] Y. Kabalci, 5G Mobile Communication Systems: Fundamentals, Challenges, and Key Technologies, Smart Grids and Their Communication Systems, Springer (2019), pp. 329-359
[11] A. Zaidi, F. Athley, J. Medbo, X. Chen, and G. Durisi, 5G physical layer: Principles, models and technology components, Academic Press, 2018.
[12] U. Mutlu, Y. Kabalci, Effects of Antenna Array on Throughput in 5G NR PDSCH, III. International Turkic World Congress on Science and Engineering (TURK-COSE), pp. 98-108, 2021
[13] E. Telatar, Capacity of multi-antenna Gaussian channels, Eur. Trans. Telecommun., vol. 10, no. 6, pp. 585–595, 1999, doi: 10.1002/ett.4460100604.
[14] M. A. Albreem, A. H. Al Habbash, A. M. Abu-Hudrouss, and S. S. Ikki, Overview of Precoding Techniques for Massive MIMO, IEEE Access, vol. 9, pp. 60764–60801, 2021, doi: 10.1109/ACCESS 2021. 3073325.
[15] T. Kebede, Y. Wondie, J. Steinbrunn, H. B. Kassa, and K. T. Kornegay, Precoding and Beamforming Techniques in mmWave-Massive MIMO : Performance Assessment, IEEE Access, vol. 10, pp. 16365–16387, 2022, doi: 10.1109/ACCESS 2022.314 9301.
[16] R. M. Asif, J. Arshad, M. Shakir, S. M. Noman, and A. U. Rehman, Energy Efficiency Augmentation in Massive MIMO Systems through Linear Precoding Schemes and Power Consumption Modeling, Wirel. Commun. Mob. Comput., vol. 2020, pp. 1–13, Sep. 2020, doi: 10.1155/2020/8839088.
[17] D. Kadhim, Promising Gains of 5G Networks with Enhancing Energy Efficiency Using Improved Linear Precoding Schemes, Int. J. Intell. Eng. Syst., vol. 14, no. 3, pp. 139–149, Jun. 2021, doi: 10.22266/ijies2021 .0630.13.
[18] J. Kaur, O. R. Popoola, M. Ali Imran, Q. H. Abbasi, and H. T. Abbas, Improving Throughput For Mobile Receivers Using Adaptive Beamforming, in 2021 1st International Conference on Microwave, Antennas & Circuits (ICMAC), Dec. 2021, pp. 1–4, doi: 10.1109 /ICMAC54080.2021.9678216.
[19] N. Fatema, G. Hua, Y. Xiang, D. Peng, and I. Natgunanathan, Massive MIMO Linear Precoding: A Survey, IEEE Syst. J., vol. 12, no. 4, pp. 3920–3931, 2018, doi: 10.1109/JSYST.2017.2776401.
[20] X. Qiao, Y. Zhang, and L. Yang, Conjugate Gradient Method Based Linear Precoding with Low-Complexity for Massive MIMO Systems, in 2018 IEEE 4th International Conference on Computer and Communications (ICCC), Dec. 2018, pp. 420–424, doi: 10.1109/CompComm.2018.8780818.
[21] B. Lee, Simplified Antenna Group Determination of RS Overhead Reduced Massive MIMO for Wireless Sensor Networks, Sensors, vol. 18, no. 2, p. 84, Dec. 2017, doi: 10.3390/s18010084.

[22] V. Ivanov, A. Medvedev, I. Bondareva and V. Grigoriev, Performance of 5G SU-MIMO Employing OFDM Bandwidth and Per-Subcarrier Precoding, Editors: O. Galinina, S. Andreev, S. Balandin, Y. Koucheryavy, Internet of Things, Smart Spaces, and Next Generation Networks and Systems. NEW2AN 2020, ruSMART 2020. https://doi.org/10.1007/978-3-030-65729-1

[23] ETSI TS 138 211 - V16.2.0, 5G NR; Physical channels and modulation (3GPP TS 38.211 version 16.2.0 Release 16), ETSI 2020

[24] M. Vu and A. Paulraj, MIMO wireless linear precoding, IEEE Signal Process. Mag., vol. 24, no. 5, pp. 86–105, 2007, doi: 10.1109/MSP.2007.904811.

[25] B. Clerckx and C. Oestges, MIMO Wireless Networks, Academic Press, 2013.

[26] A. Paulraj, R. Nabar, and D. Gore, Introduction to space-time wireless communications, Cambridge University Press, 2003.

[27] J. B. Andersen, Array gain and capacity for known random channels with multiple element arrays at both ends, IEEE J. Sel. Areas Commun., vol. 18, no. 11, pp. 2172–2178, 2000, doi: 10.1109/49.895022.

[28] ETSI TS 138 212 - V16.2.0, "5G NR; Multiplexing and channel coding (3GPP TS 38.212 version 16.2.0 Release 16), ETSI 2020

[29] ETSI TS 138 300 - V16.2.0, 5G; NR; NR and NG-RAN Overall description; Stage-2 (3GPP TS 38.300 version 16.2.0 Release 16), 2020.

[30] U. Mutlu, Y. Kabalci, Deep Learning Aided Channel Estimation Approach for 5G Communication Systems, 2022 4th Global Power, Energy and Communication Conference (GPECOM), pp. 655-660, 2022, doi: 10.1109/GPECOM55404.2022.9815811

[31] T. Dubois, M. Hélard, M. Crussière, and C. Germond, Performance of time reversal precoding technique for MISO-OFDM systems, Eurasip J. Wirel. Commun. Netw., vol. 2013, no. 1, pp. 1–16, 2013, doi: 10.1186/1687-1499-2013-260.

[32] G. Barb and M. Otesteanu, On the Influence of Delay Spread in TDL and CDL Channel Models for Downlink 5G MIMO Systems, 2019 IEEE 10th Annu. Ubiquitous Comput. Electron. Mob. Commun. Conf. UEMCON 2019, pp. 0958–0962, 2019, doi: 10.1109/UEMCON47517.2019.8992982.

[33] ETSI TR 138 900, LTE; 5G; Study on channel model for frequency spectrum above 6 GHz (3GPP TR 38.900 version 15.0.0 Release 15), 2018

[34] X. Chen, "Throughput Modeling and Measurement in an Isotropic-Scattering Reverberation Chamber," IEEE Trans. Antennas Propag., vol. 62, no. 4, pp. 2130–2139, Apr. 2014, doi: 10.1109/TAP.2014.2301850.

[35] D. Borges, P. Montezuma, R. Dinis, and M. Beko, "Massive MIMO Techniques for 5G and Beyond—Opportunities and Challenges," Electronics, vol. 10, no. 14, p. 1667, Jul. 2021, doi: 10.3390/electronics10141667.